

1 **Increased prefrontal activity with aging reflects nonspecific neural responses rather**  
2 **than compensation**

3 Alexa M. Morcom<sup>1</sup>

4 Richard N. A. Henson<sup>2</sup>, for Cambridge Centre for Ageing and Neuroscience<sup>3</sup>

5 <sup>1</sup>Centre for Cognitive Ageing and Cognitive Epidemiology, University of Edinburgh, United  
6 Kingdom

7 <sup>2</sup>MRC Cognition and Brain Sciences Unit, Cambridge CB2 3EB, United Kingdom

8 <sup>3</sup>Cambridge Centre for Ageing and Neuroscience (Cam-CAN), University of Cambridge and  
9 MRC Cognition and Brain Sciences Unit, Cambridge CB2 3EB, United Kingdom

10

11 Alexa M. Morcom can be contacted at: alexa.morcom@ed.ac.uk

12

13 No. of Figures = 3

14 No. of Tables = 5

15 No multimedia/ extended data

16

17

## 18 Abstract

19 Elevated prefrontal cortex activity is often observed in healthy older adults despite declines in  
20 their memory and other cognitive functions. According to one view, this activity reflects a  
21 compensatory functional posterior-to-anterior shift, which contributes to maintenance of  
22 cognitive performance when posterior cortical function is impaired. Alternatively, the increased  
23 prefrontal activity may be less efficient or less specific, owing to structural and neurochemical  
24 changes accompanying aging. These accounts are difficult to distinguish on the basis of  
25 average activity levels within brain regions. Instead, we used a novel model-based multivariate  
26 analysis technique, applied to two independent functional magnetic resonance imaging  
27 datasets from an adult-lifespan human sample (N=123 and N=115; approximately half  
28 female). Standard analysis replicated the age-related increase in average prefrontal  
29 activation, but multivariate tests revealed that this activity did not carry additional information.  
30 The results contradict the hypothesis of a compensatory posterior-to-anterior shift. Instead,  
31 they suggest that the increased prefrontal activation reflects reduced efficiency or specificity,  
32 rather than compensation.

## 33 Significance statement

34 Functional brain imaging studies have often shown increased activity in prefrontal brain  
35 regions in older adults. This has been proposed to reflect a compensatory shift to greater  
36 reliance on prefrontal cortex, helping to maintain cognitive function. Alternatively, activity may  
37 become less specific as people age. This is a key question in the neuroscience of aging. In  
38 this study, we used novel tests of how different brain regions contribute to long- and short-  
39 term memory. We found increased activity in prefrontal cortex in older adults, but this activity  
40 carried less information about memory outcomes than activity in visual regions. These findings  
41 are relevant for understanding why cognitive abilities decline with age, suggesting that optimal  
42 function depends on successful brain maintenance rather than compensation.

43

44

45

46

## 47 Introduction

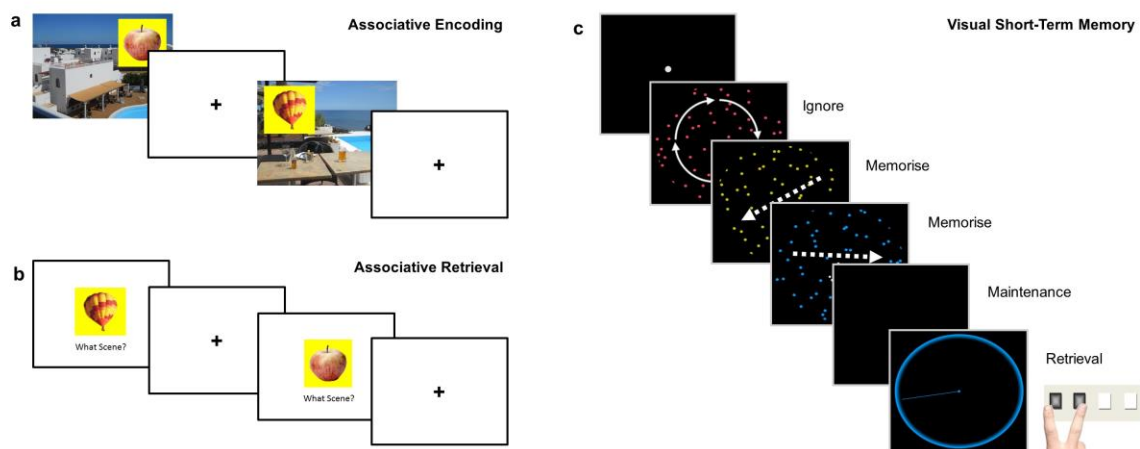
48 It is well established that healthy aging is associated with a decline in cognitive processes like  
49 memory, but mechanistic explanation of this decline is impeded by difficulties in interpreting  
50 the underlying brain changes. Functional magnetic resonance imaging (fMRI) of such  
51 cognitive processes shows striking increases, as well as decreases, in brain activity of older  
52 relative to younger adults. One leading theory – the Posterior-to-Anterior Shift in Aging (PASA)  
53 – states that recruitment of anterior regions like prefrontal cortex (PFC) contributes to  
54 maintenance of cognitive performance when posterior cortical function is impaired (Davis,  
55 Dennis, Daselaar, Fleck, & Cabeza, 2008; Grady, 2012; Park & Reuter-Lorenz, 2009).  
56 Alternatively, age-related increases in PFC activity may reflect reduced efficiency or specificity  
57 of neuronal responses, reflecting primarily age-related functional impairment within PFC  
58 (West, 1996; Glisky et al., 2001; Raz and Rodrigue, 2006; Nyberg, Lövdén, Riklund,  
59 Lindenberger, & Bäckman, 2012; Park et al., 2004). It is difficult to adjudicate between these  
60 theories based on average activity levels within brain regions (Morcom and Johnson, 2015).  
61 We used a novel multivariate approach to directly test predictions of the PASA theory.

62 With multivariate methods that examine distributed patterns of brain activity over many voxels,  
63 one can ask whether increased anterior activity provides additional information, and whether  
64 this information goes beyond that provided by posterior cortical regions. Such increases in the  
65 information represented by PFC activity would support theories that attribute additional PFC  
66 recruitment to compensatory mechanisms. We used a model-based decoding approach called  
67 multivariate Bayes (MVB) (Friston et al., 2008; Morcom and Friston, 2012; Chadwick et al.,  
68 2014), which estimates the patterns of activity that best predict a target cognitive outcome.  
69 Importantly, MVB allows formal comparison of models comprising different brain regions, such  
70 as PFC, posterior cortex, or their combination.

71 In this study, we applied MVB to fMRI data from two different paradigms in population-derived,  
72 adult-lifespan samples (N=123 and N=115, 19-88 years; Shafto et al. 2014). In the first, long-  
73 term memory (LTM) experiment, participants were scanned while encoding new memories of  
74 unique pairings of objects and background scenes, and the target cognitive outcome was  
75 whether or not these associations were subsequently remembered (Figure 1a). A previous  
76 behavioral study in an independent sample showed a strong decline in such associative  
77 memory across the adult lifespan (Henson et al., 2016). To test whether findings generalized  
78 across tasks and cognitive domains, as PASA predicts (Davis et al., 2008), we replicated our  
79 findings in a second, visual short-term memory (STM) experiment. In the STM experiment, a  
80 separate sample of participants was scanned while maintaining visual dot patterns online for  
81 a few seconds in the presence of distraction, and the target cognitive outcome was the

82 increase in the number of patterns to be maintained (i.e., load; Figure 1b). Increases in PFC  
 83 activity have frequently been reported in older adults in similar tasks (Grady et al., 1998;  
 84 Cabeza et al., 2004), although sometimes activity reductions are found at higher loads  
 85 (Cappell et al., 2010).

86 We defined two regions-of-interest (ROIs): posterior visual cortex (PVC), comprising lateral  
 87 occipital and fusiform cortex, and PFC, comprising ventrolateral, dorsolateral, superior and  
 88 anterior regions (Fig 2a). These ROIs were based on previous fMRI studies of memory tasks,  
 89 and those cited in the context of the PASA theory (Davis et al., 2008; Maillet and Rajah, 2014).



90

91 **Figure 1.** Memory tasks. a and b, long-term memory (LTM) task and c, short-term memory (STM) task.  
 92 a, Associative encoding. In the scanned Study phase of the LTM task, participants were asked to make  
 93 up a story that linked each object with its background scene (120 trials total). A scene with positive  
 94 valence is illustrated. On each trial, the scene was presented for 2 sec, then the object superimposed  
 95 for 7.5 sec, finally the screen was blanked for 0.5 sec before the next trial. b, Associative retrieval. At  
 96 Test (out of the scanner), each object was presented again, and after a measure of priming, item  
 97 memory and background valence memory, participants were asked to verbally describe the scene with  
 98 which it was paired at Study. The latter verbal recall was scored as correct or incorrect, which was then  
 99 used to classify the trials at Study into “remembered” and “forgotten” (see text for details). The example  
 100 illustrates encoding and retrieval of a trial with neutral valence. c, An example trial of STM task with  
 101 memory load of 2 items. Trials began with fixation dot for 7 sec. On each trial, three dot displays were  
 102 displayed in red, yellow and blue for 500 msec each (250 msec gap). To vary load, the dots in either  
 103 one, two or three of the dot displays moved in a consistent direction (the to-be-ignored displays rotated).  
 104 After the last display, the screen was blanked for an 8 sec maintenance period. Then the probe display  
 105 presented a colored circle to indicate which dot display to recall (red, yellow or blue). Participants had  
 106 up to 5 sec to adjust the pointer until the direction matched that of the to-be-remembered display.

107

## 108 Materials and Methods

### 109 Experiment 1: Long-term Memory Encoding

#### 110 *Participants*

111 A healthy, population-derived adult lifespan human sample (N=123; 19-88 years; 66 female)  
112 was collected as part of the Cam-CAN study (Shafto et al., 2014). Participants were fluent  
113 English speakers in good physical and mental health. Exclusion criteria included a low Mini  
114 Mental State Examination (MMSE) score ( $\leq 24$ ), serious current medical or psychiatric  
115 problems, or poor hearing or vision, as well as standard MRI safety criteria. Two participants  
116 were excluded from fMRI analysis as subsequent memory could not successfully be decoded  
117 from either region of interest (see Multivariate Bayesian decoding). Two further participants  
118 were excluded because of statistical outlier values in the analysis of univariate subsequent  
119 memory effects (see Statistics for criteria). The experiment used a within-participant design,  
120 so all participants received all the task conditions. Therefore, randomization and blinding were  
121 not required. The study was approved by the Cambridgeshire 2 (now East of England—  
122 Cambridge Central) Research Ethics Committee. Participants gave informed written consent.

#### 123 *Materials*

124 Stimuli were 160 pictures of everyday emotionally-neutral objects taken from Smith et al.  
125 (2004). For the study phase, objects were presented within a square yellow background on  
126 one of 120 scenes from the IAPS emotional pictures database (Lang et al., 1997). Scenes  
127 were grouped into 40 per valence (positive, neutral, negative), selected based on a pilot study,  
128 with the same randomized trial order for each valence condition for all participants. To control  
129 for stimulus effects, the 160 objects were divided randomly into 4 sets, and the allocation of  
130 object sets to scene valence rotated across participants in 4 different counterbalances (see  
131 Henson et al., 2016, for further details).

#### 132 *Behavioral procedure*

133 The procedure is summarized in Figure 1a. The scanned study phase comprised 120 trials,  
134 presented in two 10 min blocks separated by a short break. On each study trial, a background  
135 scene was first presented for 2 sec, and an object then superimposed for 7.5 sec, slightly  
136 above center and either to the left or right. Participants were asked to create a story that linked  
137 the object to the scene, to press a button when they had made the story. In order to equate  
138 the amount of time spent processing the story, participants were asked to continue to  
139 elaborate it until the scene and object disappeared. A blank screen of 0.5 sec was then  
140 presented prior to the next trial. Participants were informed that the task would include some

141 pleasant and unpleasant scenes. They were not told that their memory would be tested later.  
 142 A practice session of 6 study trials was given just beforehand.

143 The test phase took place outside the scanner, following a short break of approximately 10  
 144 min involving refreshment and conversation with the experimenter. The 120 objects from the  
 145 study phase were presented again, randomly intermixed with 40 new objects, and divided into  
 146 4 blocks lasting approximately 20 min each. The first stage of each test trial involved tests of  
 147 priming, item memory and memory for the picture valence (see Henson et al., 2016 for details)  
 148 However, for the present fMRI analysis, we focused on the fourth question in each trial.  
 149 Participants were asked to verbally recall the scene that had been paired with the test object  
 150 at study. Trials at study in which scenes that were correctly recalled at test, in terms of detail  
 151 or gist, were scored as “remembered”. Remaining trials were split according to whether the  
 152 scenes could not be recalled (“associative misses”), or for which an incorrect scene was  
 153 described instead (“associative intrusions”), or for which the object was not recognized (“item  
 154 misses”). Initial analyses showed no evidence that valence interacted with age, so trials were  
 155 collapsed across valence (see Behavioral results). Table 1 summarizes the trial numbers per  
 156 condition split by age tertile.

	Younger (19-45 years) n=38	Middle-Age (46-64 years) n=43	Older (65-88 years) n=42
Remembered	55 (25)	44 (24)	23 (15)
Forgotten			
Associative Miss	31 (13)	38 (17)	46 (18)
Associative Intrusion	11 (8)	13 (10)	10 (8)
Item Miss	22 (15)	25 (17)	42 (24)

157 **Table 1.** Trial numbers divided by condition. Remembered = trials with correct object recognition and  
 158 scene recall; Associative Miss = trials with correct object recognition but no scene recall; Associative  
 159 Intrusion = trials with correct object recognition but recall of an incorrect scene; Item Miss = trials with  
 160 misclassification of the object as unstudied. Data are split by age tertile. Means are given with  
 161 standard deviations (SD).

162 For the main imaging analyses, we combined the three types of forgotten trial in order to  
163 maximise power. However, in case processes that lead to subsequent memory for associative  
164 memory versus item memory differ (e.g., Dennis et al., 2008; Mattson et al., 2014), we ran a  
165 subsidiary imaging analyses with item misses excluded.

#### 166 *Imaging data acquisition and preprocessing*

167 The MRI data were collected using a Siemens 3 T TIM TRIO system (Siemens, Erlangen,  
168 Germany). MR data preprocessing and univariate analysis used the SPM12 software  
169 (Wellcome Department of Imaging Neuroscience, London, UK, [www.fil.ion.ucl.ac.uk/spm](http://www.fil.ion.ucl.ac.uk/spm)),  
170 release 4537, implemented in the AA 4.0 pipeline  
171 (<https://github.com/rhodricusack/automaticanalysis>). The functional images were acquired  
172 using T2\*-weighted data from a Gradient-Echo Echo-Planar Imaging (EPI) sequence. A total  
173 of 320 volumes were acquired in each of the 2 Study sessions, each containing 32 axial slices  
174 (acquired in descending order), slice thickness of 3.7 mm with an interslice gap of 20% (for  
175 whole brain coverage including cerebellum; TR =1970 msec; TE = 30 msec; flip angle =78  
176 degrees; field of view (FOV) =192 mm x 192 mm; voxel-size = 3 mm x 3 mm x 4.44 mm). A  
177 structural image was also acquired with a T1-weighted 3D Magnetization Prepared RAPid  
178 Gradient Echo (MPRAGE) sequence (repetition time (TR) 2250ms, echo time (TE) 2.98 ms,  
179 inversion time (TI) 900 msec, 190 Hz per pixel; flip angle 9 deg; FOV 256 x 240 x 192 mm;  
180 GRAPPA acceleration factor 2).

181 The structural images were rigid-body registered with an MNI template brain, bias-corrected,  
182 segmented and warped to match a gray-matter template created from the whole CamCAN  
183 Stage 3 sample (N=272) using DARTEL (Ashburner, 2007) (see Taylor *et al.*, 2015) for more  
184 details). This template was subsequently affine-transformed to standard Montreal  
185 Neurological Institute (MNI) space. The functional images were then spatially realigned,  
186 interpolated in time to correct for the different slice acquisition times, rigid-body coregistered  
187 to the structural image and then transformed to MNI space using the warps and affine  
188 transforms from the structural image, and resliced to 3x3x3mm voxels.

#### 189 *Univariate imaging analysis*

190 For each participant, a General Linear Model (GLM) was constructed, comprising three neural  
191 components per trial: 1) a delta function at onset of the background scene, 2) an epoch of 7.5  
192 sec which onset with the appearance of the object (2 sec after onset of scene) and offset when  
193 both object and scene disappeared, and 3) a delta function for each keypress. Each neural  
194 component was convolved with a canonical haemodynamic response function (HRF) to create  
195 a regressor in the GLM. The scene onset events were split into 3 types (i.e, 3 regressors)  
196 according to the valence of the scene on each trial, while the keypress events were modelled

197 by the same regressor for all trials (together, these four regressors served to model trial-locked  
198 responses that were not of interest). The responses of interest were captured by the epoch  
199 neural component, during which participants were actively relating the scene and object (see  
200 Behavioral Procedure). The duration of this component did not depend on response time, as  
201 participants were instructed to continue to link the object and scene mentally for the full  
202 duration of the display.

203 For the principal GLMs, the epoch component was split into 6 types (regressors) according to  
204 the 3 scene valences and 2 types of subsequent memory, i.e., study trials for which the scenes  
205 were correctly recalled (“remembered”), and those for which the scenes could not be recalled,  
206 an incorrect scene was described instead, or the object was not recognized (“forgotten”).  
207 When comparing remembered and forgotten trials, we averaged across the three valences  
208 because 1) there was no behavioral evidence of an interaction between age and valence on  
209 subsequent memory, 2) there was no imaging evidence of an interaction between age and  
210 valence on subsequent memory, and 3) there would have been insufficient numbers of each  
211 trial-type to examine each valence separately. Thus the main target contrast for the univariate  
212 and multivariate analyses were remembered versus forgotten trials.

213 As noted above, given that encoding of associative (source) information versus item  
214 information may differ with regard to additional recruitment and (potentially) to compensation  
215 (e.g., Dennis et al., 2008; Mattson et al., 2014), we ran a subsidiary analysis in which the  
216 “forgotten” category excluded item misses. In these GLMs, study trials were modelled using 9  
217 regressors according to the 3 scene valences and 3 (rather than 2) types of subsequent  
218 memory: trials on which the object was recognized but the scene forgotten or incorrectly  
219 recalled (“association forgotten”) and trials on which the object was not recognized (“item  
220 forgotten”). Participants for whom one of the sessions did not contain at least one trial of each  
221 type were removed, leaving n=109 (note this involved removal of more participants in the  
222 oldest age tertile: 0 removed aged 19-35, 2 aged 46-64, and 12 aged 65-88 years). One  
223 remaining outlier (>5 SD) on the univariate measures was removed, giving n=108. As reported  
224 in the Results section, this subsidiary analysis corroborated the findings of the main analysis.

225 Six additional regressors representing the 3 rigid body translations and rotations estimated in  
226 the realignment stage were included in each GLM to capture residual movement-related  
227 artifacts. Finally the data were scaled to a grand mean of 100 over all voxels and scans within  
228 a session, and the model was fitted to the data in each voxel. The autocorrelation of the error  
229 was estimated using an AR(1)-plus-white-noise model, together with a set of cosines that  
230 functioned to highpass the model and data to 1/128 Hz, fit using Restricted Maximum  
231 Likelihood (ReML). The estimated error autocorrelation was then used to “prewhiten” the



232 model and data, and ordinary least squares used to estimate the model parameters. To  
233 compute subsequent memory effects, the parameter estimates for the 6 epoch components  
234 were averaged across the two sessions and the three valences (weighted by number of trials  
235 per session/valence), and contrasted directly as remembered minus forgotten (Morcom et al.,  
236 2003; Maillet and Rajah, 2014). Univariate statistical analyses were conducted on the mean  
237 subsequent memory effect across all voxels in the MVB analysis, in each ROI for each  
238 participant (see next section).

## 239 Experiment 2: Visual STM

### 240 *Participants*

241 Participants were a separate subset (N=115; 25-86 years; 54 female) of those recruited to the  
242 Cam-CAN study (see Experiment 1, Participants, for details). Nineteen participants were  
243 excluded from the current analysis as the contrast of interest could not successfully be  
244 decoded from either region of interest (see Multivariate Bayesian decoding). None were  
245 excluded because of statistical outlier values on the measures used (see Statistics for criteria).  
246 The experiment used a within-participant design, so all participants received all the task  
247 conditions.

### 248 *Materials*

249 The task was adapted from Emrich et al. (2013). Stimuli were three patches of coloured dots,  
250 one red, one yellow, and one blue. Dots were 0.26 degrees of visual angle (dva) in diameter,  
251 at a density of 0.7 per square degree, and viewed through a circular aperture of diameter 11  
252 dva. As a manipulation of set size, one, two, or three of the dot displays moved (at 2 dva/ sec)  
253 in a single direction which had to be remembered. The other, distractor, displays rotated  
254 around a central axis, and were be ignored. On 90% of trials the probed movements were in  
255 one of three directions (7, 127, or 247 degrees). Other directions were selected at random, to  
256 avoid subjects learning the target directions. Order of presentation of the 3 display colors was  
257 randomized trial by trial, as was memory load. Rotation direction alternated across trials of a  
258 given load.

### 259 *Behavioral procedure*

260 Each trial began with a grey fixation dot in the middle of a black screen for 5 sec, which then  
261 turned white for 2 sec. Participants then saw the 3 dot displays for 500 msec each, with 250  
262 msec in-between. After the third display, an 8 sec blank fixation delay was presented, followed  
263 by the probe display. The probe display showed a colored circle to indicate which dot display  
264 to recall (red, yellow, or blue), with a pointer. Participants had up to 5 sec to adjust the pointer  
265 using 2 buttons until it matched the direction of motion of the remembered target dot display.

266 After responding, a third button cleared the probe display. Participants completed 3 runs of 30  
267 trials per run (10 for each load). The direction of the target, the sequential position of the target,  
268 and the set size were counterbalanced within each run, and presented in random order. Colour  
269 and position of target were also counterbalanced using a Greco-Latin square design.

### 270 *Imaging data acquisition and preprocessing.*

271 Imaging data were acquired on the same scanner as Experiment 1. Functional T2\*-weighted  
272 data were acquired using a Multi-Echo Gradient-Echo Echo-Planar Imaging (EPI) sequence.  
273 Approximately 300 volumes were acquired in each of the 3 VSTM task sessions (duration  
274 depending on response times). Each volume had 34 axial slices (acquired in descending  
275 order), slice thickness of 2.9 mm with an interslice gap of 20% (FOV = 224 mm × 224 mm, TR  
276 = 2000 msec; TE = 12 msec, 25 msec, 38 msec; flip angle = 78 degrees; voxel-size = 3.5 mm  
277 × 3.5 mm × 3.48 mm). Structural image sequences were the same as in Experiment 1. The  
278 multiple echos were combined by computing their average, weighted by their estimated T2\*  
279 contrast. The functional images were spatially realigned and interpolated in time to correct for  
280 different slice acquisition times. Spatial normalisation used the 'new segment' protocol in  
281 SPM12 (Ashburner and Friston, 2005). Participants' structural scans were coregistered to their  
282 mean functional image, then segmented into 6 tissue classes. Functional images were rigid-  
283 body coregistered to the structural image then transformed to MNI space using the warps and  
284 affine transforms estimated from the structural image, and resliced to 2x2x2mm voxels.

### 285 *Univariate imaging analysis*

286 The GLM for each participant comprised three neural components per trial: 1) encoding,  
287 modelled as an epoch of 1 sec duration at onset of the first moving dot pattern, 2)  
288 maintenance, modelled as an epoch of 4 sec at offset of the last moving dot pattern (2.25 sec  
289 after onset of 1), and 3) probe, a delta function at the time of the participant's response. These  
290 components were each split into 3 types (regressors) according to the 3 STM load levels. As  
291 in Experiment 1, 6 additional regressors were added representing the motion parameters  
292 estimated in the realignment stage. Finally the data were scaled to a grand mean of 100 over  
293 all voxels and scans within a session. To confirm that this dataset was suitable as a replication  
294 of Experiment 1's multivariate results, we first checked that at least one significant cluster  
295 within the PFC region of interest (ROI) showed increased univariate activity in older people.  
296 This was done using a standard analysis of effects of a linear contrast of increasing VSTM  
297 load on activity during the delay period, whole-brain corrected for multiple comparisons at  $p <$   
298  $.05$  (voxel threshold), and a linear contrast of age. Details of this analysis are not reported and  
299 it did not contribute to ROI selection, which was the same as for Experiment 1. Note that the  
300 continuous nature of the judgment in the VSTM task precludes definition of individual trials as

301 correct or incorrect (rather, performance is used to estimate continuous summary measures  
302 for each participant, as in Emrich et al, 2013). Therefore all trials were included in the fMRI  
303 analysis, and the main target contrast for the univariate and multivariate analyses was the  
304 linear effect of load from 1-3 during the delay period.

#### 305 Regions of interest

306 ROIs were defined using WFU PickAtlas ([http://fmri.wfubmc.edu/\\_version\\_3.0.5](http://fmri.wfubmc.edu/_version_3.0.5)) with AAL and  
307 Talairach atlases (Lancaster et al., 2000; Tzourio-Mazoyer et al., 2002; Maldjian et al., 2003).  
308 The posterior visual cortex (PVC) mask comprised bilateral lateral occipital cortex and fusiform  
309 cortex (from AAL, fusiform and middle occipital gyri), and the PFC mask comprised bilateral  
310 ventrolateral, dorsolateral, superior and anterior regions: from AAL, the inferior frontal gyrus  
311 (IFG), both pars triangularis and pars orbitalis; middle frontal gyrus, lateral part (MFG);  
312 superior frontal gyrus (SFG); and from Talairach, Brodmann Area 10 (BA10), dilation factor =  
313 1. In the subregion analyses, separate masks were created for BA10, IFG, MFG and SFG  
314 (regions included in the BA10 mask were excluded from the other masks).

#### 315 Multivariate Bayesian decoding

316 A series of MVB decoding models were fit to assess the information about subsequent  
317 memory carried by individual ROIs or combinations of ROIs. Each MVB decoding model is  
318 based on the same design matrix of experimental variables used in the univariate GLM, but  
319 the mapping is reversed: many physiological data features (derived from fMRI activity in  
320 multiple voxels) are used to predict a psychological target variable (Friston et al., 2008). This  
321 target (outcome) variable is specified as a contrast. In Experiment 1 (LTM) the outcome was  
322 subsequent memory, and in Experiment 2 (STM) it was the linear increase in STM load during  
323 maintenance periods. Modelled confounds in the design (all covariates apart from those  
324 involved in the target contrast) are removed from both target and predictor variables.

325 Each MVB model is fit using hierarchical parametric empirical Bayes, specifying empirical priors  
326 on the data features (voxel-wise activity) in terms of patterns over voxel features and the  
327 variances of the pattern weights. Since decoding models operating on multiple voxels (relative  
328 to scans) are ill-posed, these spatial priors on the patterns of voxel weights act as constraints  
329 in the second level of the hierarchical model. MVB also uses an overall sparsity (hyper) prior  
330 in pattern space which embodies the expectation that a few patterns make a substantial  
331 contribution to the decoding and most make a small contribution. The pattern weights  
332 specifying the mapping of data features to the target variable are optimised with a greedy  
333 search algorithm using a standard variational scheme which iterates until the optimum set size  
334 is reached (Friston et al., 2007). This is done by maximizing the free energy, which provides

335 an upper bound on the Bayesian log-evidence (the marginal probability of the data given that  
 336 model). The evidence for different models predicting the same psychological variable can then  
 337 be compared by computing the difference in their log-evidences, giving the log (marginal)  
 338 likelihood ratio test (Bayes factor) (see Friston et al., 2007; Chadwick et al., 2012; Morcom  
 339 and Friston, 2012). In this work, the main outcome measures were the log-evidence for each  
 340 model and the set of fitted weights for all patterns (voxels) in the ROI, which can be examined  
 341 to assess their distribution over voxels and the contributions of different combinations of  
 342 voxels. These analyses were implemented in SPM12 v6486 and custom MATLAB scripts.

343 Features (voxels) for MVB analysis were selected using an orthogonal contrast and a leave-  
 344 one-participant-out scheme. For each participant and ROI, these were the 1000 voxels with  
 345 the strongest responses to the task: in Experiment 1 (LTM), the 6 epoch regressors modelling  
 346 object onsets in the GLM, and in Experiment 2 (STM), the 3 epoch regressors modelling  
 347 maintenance periods in the GLM (defined using an F contrast in all other participants testing  
 348 variance explained by these regressors, regardless of valence or subsequent memory). We  
 349 used a sparse spatial prior, in which each pattern is an individual voxel (Morcom and Friston,  
 350 2012; Chadwick et al., 2014; Hulme et al., 2014; Maass et al., 2014). We first checked that  
 351 the target memory variables could reliably be decoded from the selected features by  
 352 contrasting the evidence for each model with the evidence for models in which the design  
 353 matrix (and therefore the target variable) had been randomly phase-shuffled, taking the mean  
 354 over 20 repetitions, and comparing log-evidence for real versus phase-shuffled models. One-  
 355 tailed *t*-tests compared the difference in real versus shuffled model evidences to a  
 356 hypothesized population mean difference of 3 which would reflect good Bayesian evidence for  
 357 the real over the shuffled models. These showed that the difference in log-evidence was  
 358 robustly greater than this in both PVC,  $t(118) = 6.08$ ,  $p < .0001$ ,  $r^2_{adj} = .225$ , mean difference =  
 359 9.72; and PFC,  $t(118) = 7.70$ ,  $p < .0001$ ,  $r^2_{adj} = .323$ , mean difference = 11.8. The same applied  
 360 to Experiment 2: for PVC,  $t(95) = 8.42$ ,  $p < .0001$ ,  $r^2_{adj} = .415$ , mean difference = 23.0, and  
 361 PFC,  $t(95) = 11.4$ ,  $p < .0001$ ,  $r^2_{adj} = .569$ , mean difference = 35.0. To confirm that the sparse  
 362 prior represented the best spatial model, we then compared the log-evidence with that for  
 363 models with smooth spatial priors, in which each pattern is a local weighted mean of voxels  
 364 (Gaussian FWHM = 8). For Experiment 1 (LTM): log evidence was substantially greater for  
 365 the sparse priors in both ROIs: in PVC,  $t(118) = 18.4$ ,  $p < .0001$ ,  $r^2_{adj} = .737$ , and PFC,  $t(118)$   
 366  $= 18.0$ ,  $r^2_{adj} = .728$ ,  $p < .0001$ , two-tailed tests. The same was true for Experiment 2 (STM): for  
 367 PVC,  $t(95) = 10.3$ ,  $r^2_{adj} = .464$ ,  $p < .0001$ , and PFC,  $t(95) = 14.9$ ,  $r^2_{adj} = .650$ ,  $p < .0001$ .

368 Unlike univariate activation measures such as subsequent memory effects, but like other  
 369 pattern-information methods, MVB finds the best non-directional model of activity predicting  
 370 the target variable, so positive and negative pattern weights are equally important. Therefore,

371 the principle MVB measure of interest for each ROI was the spread (standard deviation) of the  
372 weights over voxels, reflecting the degree to which multiple voxels carried substantial  
373 information about subsequent memory. To test whether PFC activity was compensatory, we  
374 also constructed a novel measure of the contribution of prefrontal cortex to subsequent  
375 memory. This used Bayesian model comparison within participants to assess whether a joint  
376 PVC-PFC model boosted prediction of subsequent memory relative to a PVC-only model. The  
377 PASA hypothesis, in which PFC is engaged to a greater degree in older age and this  
378 contributes to cognitive outcomes, predicts that a boost will be more often observed with  
379 increasing age. The initial dependent measure was the log model evidence, coded  
380 categorically for each participant to indicate the outcome of the model comparison. The 3  
381 possible outcomes were: a boost to model evidence for PVC-PFC relative to PVC models, i.e.,  
382 better prediction of subsequent memory (difference in log evidence  $> 3$ ), equivalent evidence  
383 for the two models ( $-3 < \text{difference in log evidence} < 3$ ), or a reduction in prediction of  
384 subsequent memory for PFC-PVC relative to PVC (difference in log evidence  $< -3$ ).

385 Lastly, given that the relative contribution of anterior versus posterior regions could change  
386 with age, even if the absolute amount of pattern information decreased with age in both  
387 regions, we computed a second novel measure: we estimated the PFC contribution to  
388 cognitive outcome in terms of the proportion of top-weighted voxels in the joint PVC-PFC  
389 model that were located in PFC, as opposed to PVC, derived from joint PVC-PFC models. In  
390 each participant, the voxels making the strongest contribution to the cognitive outcome,  
391 defined as those with absolute voxel weight values greater than 2 standard deviations from  
392 the mean, were split according to their anterior versus posterior location. The dependent  
393 measure was the proportion of these top voxels located in PFC.

#### 394 Experimental design and statistical analysis

395 Sample size was determined by the initial considerations of Stage 3 of the CamCAN study –  
396 see Shafto et al. (Shafto et al., 2014) for details. For the LTM experiment, a sensitivity analysis  
397 indicated that with  $N=123$ , we would have 80% power to detect a small to medium effect  
398 explaining 6.5% of the variance on a two tailed test for a model with 2 predictors ( $r^2 = .0658$ ).  
399 For the STM experiment with  $N = 115$ , the corresponding minimal effect size for 80% power  
400 was 6.9% of the variance ( $r^2 = .0694$ ). In our previous report of aging and successful memory  
401 encoding, an *a priori* test of a between-region difference in subsequent memory effects  
402 according to age showed a large effect ( $r^2 = .257$ ) (Morcom et al., 2003).

403 Age effects on continuous multivariate or univariate dependent measures were tested using  
404 robust second-order polynomial regression with “rlm” in the package MASS for R (Venables  
405 et al., 2002); MASS version 7.3-45; R version 3.3.1) with standardized linear and quadratic

406 age predictors. For analysis of covariance for behavioral data we used JASP version 0.8.3.1.  
407 Analysis of outcomes of the between-region MVB model comparison (PVC and PFC combined  
408 versus PVC, see Fig 2 and main text) used ordinal regression with “polr” in MASS.  
409 Distributions were also trimmed to remove extreme outliers (> 5 SD above or below the mean).  
410 In Experiment 1 (LTM), the two participants (aged 72 and 80) with outlier values for univariate  
411 effects were also removed from the MVB analyses so the samples examined were  
412 comparable. We excluded two further participants (aged 68 and 83) in whom subsequent  
413 memory could not be decoded from at least one of the two ROIs (log model evidence  $\leq 3$ ),  
414 giving  $n=119$ . In Experiment 2 (STM), we excluded nineteen participants in whom VSTM load  
415 could not be decoded during maintenance, giving  $n=96$ . All tests were two-tailed and used an  
416 alpha level of .05.

417 Where it was important to test for evidence for the null hypothesis over an alternative  
418 hypothesis, we supplemented null-hypothesis significance tests with Bayes Factors  
419 (Wagenmakers, 2007; Rouder et al., 2009). The Bayes Factors were estimated using Dienes’  
420 online calculator (Dienes, 2014) which operationalizes directional hypotheses such as PASA  
421 in terms of a half-normal distribution. Here, we assumed an effect size of 1 SD and therefore  
422 defined the half-normal distribution with mean=0 and SD=1. All statistics and p values are  
423 reported to 3 significant figures, except where  $p < .0001$ .

## 424 Results

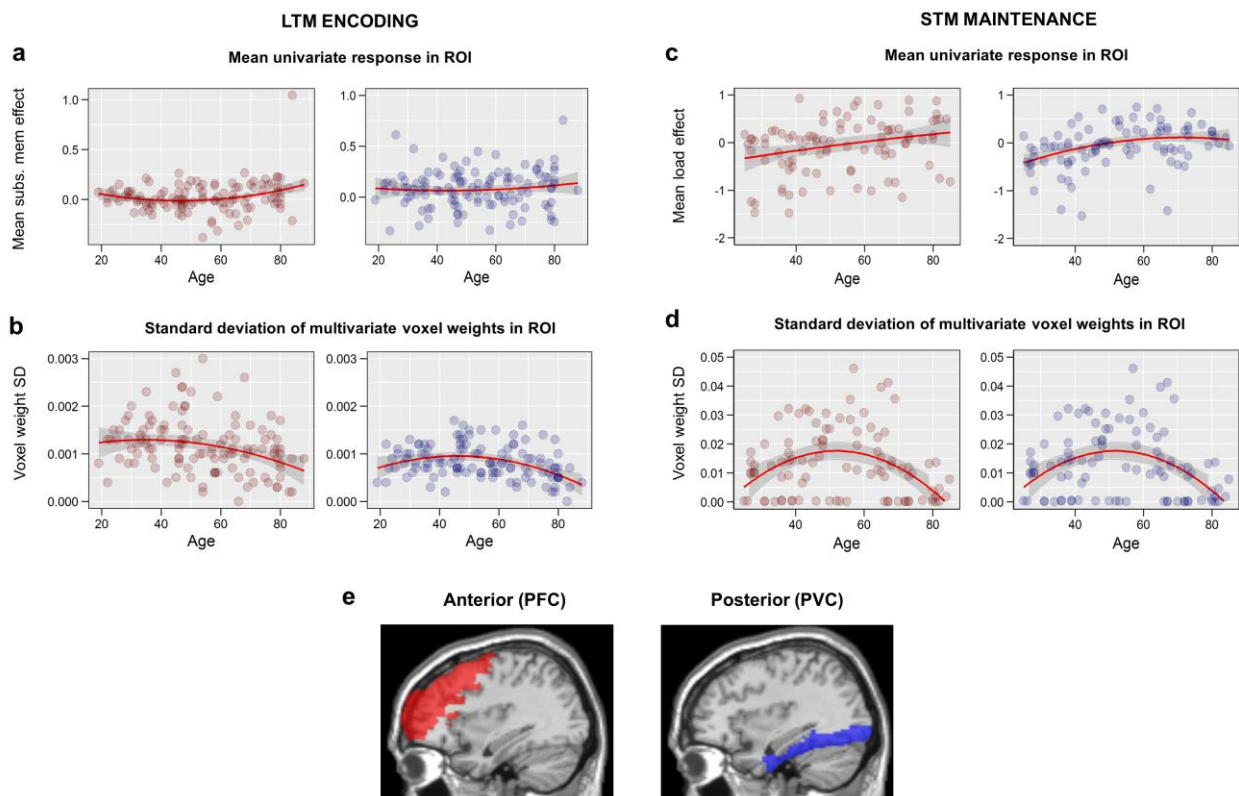
### 425 Experiment 1: Long-term Memory (LTM) Encoding

#### 426 *Behavioral results*

427 We examined age effects on the number of trials in each remembered and forgotten condition  
428 (see Table 2). For remembered trials, there was a significant linear decrease with age ( $t(118)$   
429  $= -7.30$ ,  $p < .0001$ ,  $r^2_{adj} = .299$ ), with no significant quadratic component ( $t(118) = -0.104$ ,  $p =$   
430  $.917$ ; alpha = .0125). As a consequence, the number of forgotten trials increased with age,  
431 and this was true for both associative misses (linear  $t(118) = 4.82$ ,  $p < .0001$ ,  $r^2_{adj} = .150$ ;  
432 quadratic,  $t(118) = 0.630$ ,  $p = .532$ ) and item misses (linear  $t(118) = 5.43$ ,  $p < .0001$ ,  $r^2_{adj} =$   
433  $.186$ ; quadratic,  $t(118) = 1.57$ ,  $p = .120$ ), although not for associative intrusions (linear  $t(118)$   
434  $= -1.38$ ,  $p = .163$ ; quadratic,  $t(118) = -2.29$ ,  $p = .0221$ ). Analysis of covariance with the factor  
435 of valence (Positive, Neutral, Negative) showed no interaction between age and valence on  
436 the number of remembered items (for linear effect of age,  $F(2,231) < 1$ ,  $p = .486$ ; quadratic,  
437  $F(2,231) = 1.59$ ,  $p = .206$ ).

#### 438 *Testing compensation*

439 Standard univariate activation analyses assessed mean activity in each ROI across all voxels  
 440 included in the multivariate analysis (see Materials and Methods). Consistent with the PASA  
 441 account, the increase in activity associated with subsequent memory became more  
 442 pronounced with age, particularly in later years (linear effect of age,  $t(118) = 2.43$ ,  $p = .0166$ ;  
 443 quadratic effect of age,  $t(118) = 2.58$ ,  $p = .0111$ ) (Fig 2a, Table 2). Age effects in PVC were  
 444 not significant (see Table 2). The age effects in PFC were also present after removal of the  
 445 older participant with the largest SM effect (although they did not meet our criterion for an  
 446 outlier; see Fig 2a; linear  $t(117) = 2.14$ ,  $p = .033$ ; quadratic  $F(117) = 2.31$ ,  $p = .033$ ). In both ROIs  
 447 results were very similar for the models excluding forgotten trials for which the items  
 448 themselves were forgotten (see Methods; PFC: linear  $t(107) = 2.22$ ,  $p = .0316$ ; quadratic  $t(107)$   
 449  $= 2.91$ ,  $p = .00527$ ; PVC: linear,  $t(107) = 1.10$ ,  $p = .288$ ; quadratic,  $t(107) = 1.24$ ,  $p = .233$ ).



450

451 **Figure 2.** Relationship between age and univariate and multivariate effects within ROIs. **(a).** Univariate  
 452 subsequent memory effects (mean activity for remembered - forgotten), showing increased activity with  
 453 age in PFC but not PVC. **(b).** Spread of multivariate responses predicting subsequent memory  
 454 (standard deviation of fitted MVB voxel weights), showing reduced spread of responses with age in both  
 455 ROIs. **(c).** Univariate effects of load (positive linear contrast) during STM maintenance, showing  
 456 increased activity with age in both ROIs. **(e).** Spread of multivariate responses during STM maintenance  
 457 predicting increasing load, showing reduced spread of responses with age in both ROIs. Red and blue  
 458 lines are robust-fitted second-order polynomial regression lines and shaded areas show 95%

459 confidence intervals. **(e)**. PVC (blue) and PFC (red) ROIs overlaid on sagittal section ( $x=+36$ ) of a  
 460 canonical T1 weighted brain image. Note that y-axis scales are not comparable across tasks.  
 461

ROI/ measure	Model		Linear			Quadratic		
	<i>F</i>	<i>p</i>	<i>t</i>	$r^2_{adj}$	<i>p</i>	<i>T</i>	$r^2_{adj}$	<i>p</i>
Mean univariate SM activation								
PFC	5.49	.00525	2.43	.0312	0.0166	2.58	.0371	.0111
PVC	0.426	.654	0.728	--	0.480	0.703	--	.495
PFC-PVC	0.837	.436	0.883	--	0.388	1.084	--	0.293
Multivariate spread (SD) of SM activity								
PFC	6.36	.00240	-3.33	.0701	.000998	-1.44	--	.151
PVC	11.3	< .0001	-3.49	.0780	.000650	-3.50	.0784	.000621
PFC-PVC	2.02	.109	4.16	--	.0437	.398	--	.690

462 **Table 2.** Age effects on mean univariate SM effects and spread of multivariate SM effects in the LTM  
 463 task. PFC-PVC refers to analyses where the dependent variable was the difference in each measure  
 464 between PFC and PVC. SD = standard deviation.  $r^2_{adj}$  = the unbiased estimate of the amount of variance  
 465 explained in the population.  $n = 119$ .

466

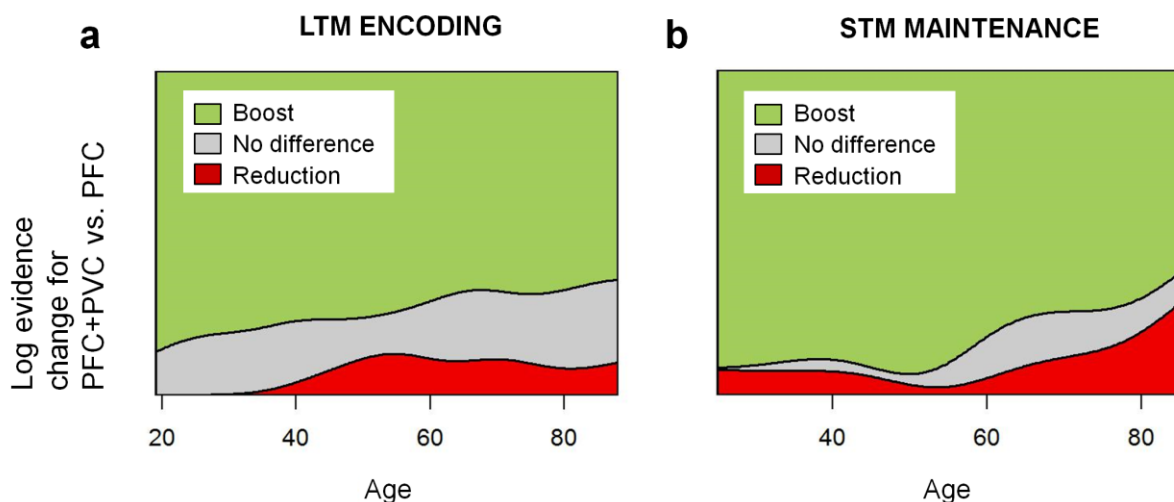
467 If the increasing PFC activation with age reflected compensation, we expected the multivariate  
 468 analyses to show that this increased activity carried additional information about subsequent  
 469 memory. However, the data revealed a different pattern. In MVB models, like other linear  
 470 models with multiple predictors, each voxel within an ROI has a weight that captures the  
 471 unique information it contributes (in this case, for predicting subsequent memory). Because  
 472 both positive and negative weights carry information, we summarised the MVB results by the  
 473 spread (standard deviation) of weights over voxels (see Materials and Methods).

474 In both ROIs, this spread was markedly reduced during later life (PVC: linear  $t(118) = -3.49$ ,  
 475  $p = .000650$ ; quadratic  $t(118) = -3.50$ ,  $p = .000621$ ; PFC: linear  $t(118) = -3.33$ ,  $p = .000998$ ;  
 476 quadratic  $t(118) = -1.44$ ,  $p = .151$ ); see Fig 2b and Table 2. This means that, contrary to a  
 477 compensatory PASA shift, PFC showed fewer, rather than more, voxels with large positive or  
 478 negative weights with increasing age. Again, the results were similar for the subsidiary models  
 479 excluding item misses (PVC: linear  $t(107) = -1.41$ ,  $p = .158$ ; quadratic  $t(107) = -2.81$ ,  $p =$   
 480  $.000544$ ; PFC: linear  $t(107) = -2.21$ ,  $p = .0280$ ; quadratic  $t(107) = -0.566$ ,  $p = .570$ ). By contrast,  
 481 the spread of univariate activities across voxels increased with age in both ROIs (for PVC,  
 482 linear effect of age,  $t(118) = 5.91$ ,  $p < .0001$ ,  $r^2_{adj} = .215$ ; quadratic effect of age,  $t(118) = 1.72$ ,



483  $p = .0881$ ; for PFC, linear effect of age,  $t(118) = 5.64$ ,  $p < .0001$ ,  $r^2_{adj} = .199$ ; quadratic  $t(118)$   
 484  $= -2.31$ ,  $p = .0226$ ,  $r^2_{adj} = .0268$ ).

485 To provide a more direct test for a compensatory posterior-to-anterior shift, we assessed the  
 486 *specific* contribution of PFC to subsequent memory, over and above that of PVC. We fitted a  
 487 joint MVB model that included both posterior and anterior ROIs, and contrasted this with a  
 488 model including PVC only, using Bayesian model comparison. Thus we could ask, for each  
 489 participant, whether or not adding PFC to the model “boosted” prediction of subsequent  
 490 memory (see Methods). Contrary to the PASA theory of a compensatory shift towards greater  
 491 reliance on PFC, a Bayes Factor comparing these two models revealed strong evidence for  
 492 the null hypothesis of no boost ( $BF_{01} = 11.1$ ); indeed, the probability of a boost to model  
 493 evidence for PVC-PFC compared to PVC-only actually *decreased* with age numerically (Fig  
 494 3a; linear  $t(118) = -1.54$ ,  $p = .126$ ). Excluding item misses from the model enhanced this  
 495 pattern (for linear age effect  $t(107) = -2.34$ ,  $p = .0211$ ,  $BF_{01} = 14.3$ ).



496

497 **Figure 3.** Evidence against a compensatory posterior-to-anterior shift from MVB comparisons between  
 498 ROIs. Ordinal regression of Bayesian model comparison of combined PVC+PFC model versus PVC-  
 499 only model using age to predict outcomes of model comparison: adding PFC to the model boosts  
 500 prediction of the cognitive outcome (difference in log-evidence  $> 3$ ), or there is no boost ( $-3 < \text{difference}$   
 501  $< 3$ ), or a reduction in log-evidence (difference  $< -3$ ). (a) LTM, for subsequent memory effects, a boost  
 502 was no more frequent with increasing age (b) STM, for load effects, a boost was less frequent with  
 503 increasing age.

#### 504 *Testing sub-regions within PFC*

505 We also explored whether the pattern of results was similar across subregions within PFC.  
 506 The PASA theory does not specify which areas are involved in a compensatory shift, but aging  
 507 does not affect all subregions equally (Raz and Rodrigue, 2006). In functional studies,

508 univariate SM effects in ventrolateral and dorsolateral PFC tend to be age-invariant while  
 509 anterior and superior prefrontal regions show age-related increases (Morcom et al., 2003;  
 510 Maillet and Rajah, 2014). In contrast, Davis et al.'s (2008) PASA proposal was based on  
 511 increased activation in older people in anterior ventrolateral PFC and anterior cingulate during  
 512 visual perception and episodic retrieval. In the present episodic encoding task, there were  
 513 significant age-related increases in univariate activation in anterior PFC (BA10) and lateral  
 514 inferior frontal gyrus (IFG), and significant decreases in the spread of multivariate voxel  
 515 weights in BA10 and superior (medial) frontal gyrus (SFG), as well as numerical decreases  
 516 also in IFG and in lateral middle frontal gyrus including dorsolateral PFC (MFG) (Table 3; see  
 517 Materials and Methods, Regions of Interest for region definition). Thus the overall age-related  
 518 increase in activation was mainly driven by BA10 and IFG, but no subregion showed a  
 519 decrease in activation with age. The reduction in multivariate information and evidence against  
 520 a functional boost were relatively uniform over subregions (Table 3). Direct model comparison  
 521 showed no evidence that PFC activity was compensatory in older age, even in the two  
 522 subregions with strong increases in activation: Bayes Factors weighed against any boost to  
 523 prediction of subsequent memory for joint PFC-PVC models relative to PVC-only models ( $BF_{01}$   
 524 favoring the null over positive linear effect of age = 11.1 for BA10, 12.5 for MFG, 5.00 for IFG  
 525 and 14.2 for SFG).

ROI/ measure	Model		Linear			Quadratic		
	<i>F</i>	<i>p</i>	<i>t</i>	$r^2_{adj}$	<i>p</i>	<i>t</i>	$r^2_{adj}$	<i>p</i>
<b>BA10</b>								
Mean univariate SM	5.24	.00660	1.33	--	.180	2.36	--	.0189
MVB spread (SD)	8.28	.000433	-3.75	.0911	.00032	-1.86	--	.0623
PFC boost	--	--	-1.44	--		-0.321	--	
<b>IFG</b>								
Mean univariate SM	5.39	.00572	2.48	.204	.0152	2.72	.227	.00824
MVB spread (SD)	3.30	.0405	-2.50	--	.0127	-0.653	--	.514
PFC boost	--	--	0.00665	--		-0.210	--	
<b>MFG</b>								
Mean univariate SM	1.34	.266	1.56	--	.119	1.38	--	.169
MVB spread (SD)	4.54	.0126	-2.86	.0487	.00466	-1.10	--	.271
PFC boost	--	--	-1.45	--		-0.132	--	
<b>SFG</b>								
Mean univariate SM	1.72	.184	1.33	--	.181	1.34	--	.179
MVB spread (SD)	4.39	.0145	-2.83	.0474	.00533	-1.09	--	.275
PFC boost	--	--	-1.68	--		1.03	--	

526 **Table 3.** Age effects for PFC subregions in the LTM task. The table lists mean univariate SM effects,  
 527 the spread (SD) of multivariate Bayesian (MVB) voxel weights predicting SM, and results of the  
 528 between-region tests of 'boost' to model evidence for PFC plus PVC models compared to PVC-only.  
 529 See text for details. Alpha = .0125. SD = standard deviation. SM = subsequent memory. n=119.

530 *Testing posterior-anterior shift*

531 The foregoing analyses provide strong evidence that the increase in (univariate) PFC activity  
 532 observed in this task did not reflect compensation. Nonetheless, the PASA theory is more  
 533 general, describing a shift in relative reliance on posterior and anterior regions with age, which  
 534 need not be compensatory, but could reflect differential age effects in posterior and anterior  
 535 cortices. In other words, the relative involvement of anterior versus posterior regions could  
 536 increase with age, even if the absolute involvement of both decreased with age. Direct  
 537 comparison of the mean univariate activation between ROIs did not reveal any evidence for  
 538 such relative differences in age effects, with strong Bayesian evidence against the predicted  
 539 greater age-related increase in PFC ( $BF_{01}$  for null hypothesis = 25; Table 2). We next tested  
 540 for a shift in the relative multivariate information between regions. In the separate MVB  
 541 models, the age-related reduction in spread of weights was numerically *greater* in PFC than  
 542 PVC (linear age effect on PFC-PVC difference,  $t(118) = 4.16$ ,  $p = .0437$ ); see Table 2. We  
 543 also measured the proportion of top-weighted voxels ( $> 2$  standard deviations above the  
 544 mean) that were located in PFC as opposed to PVC in the joint PVC-PFC model. This  
 545 proportion decreased significantly with age (overall model,  $F(2,116) = 3.27$ ,  $p = .0415$ ; linear  
 546  $t(118) = -2.55$ ,  $r^2_{adj} = .359$ ,  $p = .0119$ ; quadratic  $t(118) = -.106$ ,  $p = .915$ ), with mean 52.4% of  
 547 top voxels located in PFC in the younger tertile (SD = 9.09; 18-45 years) and 47.1% in the  
 548 older tertile (SD = 8.57; 65-88 years), although this was no longer significant when item misses  
 549 were excluded (overall model,  $F(2,105) = 2.60$ ,  $p = .0799$ , linear  $t(107) = -1.86$ ,  $p = .0638$ ).  
 550 Thus, there was no evidence that in older age there is a general shift in the areas contributing  
 551 to subsequent memory from posterior to anterior (though see Experiment 2 below).

552 Experiment 2: Short-term Memory (STM) Maintenance

553 *Behavioral results*

554 For the visual STM task, analysis of the effects of increasing load on performance showed a  
 555 strong age-related increase in the effect of load on accuracy, measured using the root mean  
 556 squared error of the estimated dot direction relative to the actual dot direction in degrees (Fig  
 557 1b). As expected, older people showed a larger increase in error at load = 3 compared to load  
 558 = 1 (linear contrast) than younger people (for linear age-by-load interaction,  $t(95) = 5.53$ ,  $p <$   
 559  $.0001$ ,  $r^2_{adj} = .192$ ; quadratic  $t(95) = 1.27$ ,  $p = .203$ ), although some age-related decrement in  
 560 accuracy was present even at load = 1 (for linear effect of age,  $t(95) = 2.607$ ,  $p = .0110$ ,  $r^2_{adj} =$   
 561  $.0382$ ; quadratic  $t(95) = 0.388$ ,  $p = .699$ ).

562 *Testing compensation*

563 For STM, standard univariate activation analyses showed that increasing load elicited activity  
 564 increases during the maintenance period which varied according to age in both ROIs. As in  
 565 the LTM experiment, and consistent with the PASA account, PFC activation increased with  
 566 age, particularly in later years (linear  $t(95) = 3.01$ ,  $p = .003$ ; quadratic  $t(95) = -0.505$ ,  $p = .615$ )  
 567 (Fig 2c, Table 4). Unlike for LTM encoding, there was also a significant increase in load-related  
 568 PVC activation over the lifespan (linear  $t(95) = 4.28$ ,  $p < .0001$ ; quadratic  $t(93) = -0.988$ ,  $p =$   
 569  $.324$ ; see Table 4.

ROI/ measure	Model		Linear			Quadratic		
	<i>F</i>	<i>p</i>	<i>t</i>	$r^2_{adj}$	<i>p</i>	<i>T</i>	$r^2_{adj}$	<i>p</i>
Mean univariate STM activation								
PFC	4.57	.0128	3.01	.0553	.00336	-0.505	--	.615
PVC	9.43	.000187	4.28	.119	< .0001	-0.988	--	.324
PFC-PVC	.606	.548	-0.587	--	.559	-0.878	--	.380
Multivariate spread (SD) of STM activity								
PFC	13.4	< .0001	.662	--	.507	-5.03	.162	< .0001
PVC	9.30	.000210	-1.01	--	.308	-4.07	.108	< .0001
PFC-PFC	3.00	.0547	.674	--	.497	2.26	.0250	.0244

570 **Table 4.** Age effects on mean univariate SM effects and spread of multivariate SM effects in the STM  
 571 task. PFC-PVC refers to analyses where the dependent variable was the difference in each measure  
 572 between PFC and PVC. SD = standard deviation.  $n = 96$ .  $R^2_{adj}$  = the unbiased estimate of the amount  
 573 of variance explained in the population.

574

575 Separate MVB analysis in each ROI showed a similar pattern of age effects to the LTM task.  
 576 In both PFC and PFC, the spread (SD) of individual voxel weights predicting increased STM  
 577 load was particularly reduced during later life, with a significant quadratic component (PVC:  
 578 linear  $t(95) = -1.01$ ,  $p = .308$ ; quadratic  $t(95) = -4.07$ ,  $p < .0001$ ; PFC: linear  $t(95) = 0.662$ ,  $p =$   
 579  $.507$ ; quadratic  $t(95) = -5.03$ ,  $p < .0001$ ) (see Fig 2d and Table 4). The result for PVC was  
 580 unchanged by removing a subset of subjects with very low values (i.e., SD weights  $< .0005$ ;  
 581 for quadratic age effect  $t(69) = -5.32$ ,  $p = .0012$ ). As found for LTM encoding, the direction of  
 582 the effect in PFC was contrary to a compensatory PASA shift, i.e., PFC voxels contributed  
 583 less to the cognitive task in old age. Again, the spread of univariate effects did not show the

584 same effects of age (in PVC linear  $t(95) = 1.52$ ,  $p = .134$ ; quadratic  $t(95) = 0.831$ ,  $p = .406$ ; in  
585 PFC, linear  $t(95) = -0.471$ ,  $p = .641$ ; quadratic  $t(95) = 1.70$ ,  $p = .0912$ ).

586 As for LTM encoding, we used model comparison of a joint PVC-PFC model with a PVC-only  
587 model to directly evaluate the compensatory PASA hypothesis. The results were similar to the  
588 LTM experiment: The “boost” to prediction of the cognitive variable obtained by adding PFC  
589 to the model showed a significant age-related *reduction* in the probability of a boost for STM  
590 load (in an ordinal regression,  $t(95) = -2.00$ ,  $p = .0479$ ). The Bayes Factor provided strong  
591 evidence against the compensatory hypothesis of an increased boost (for unidirectional  
592 hypothesis,  $BF = 10.2$ ), although evidence was only anecdotal for the presence of an age-  
593 related reduction in boost (for bidirectional hypothesis,  $BF = 1.81$ ). Thus, like for the LTM  
594 experiment, there was clear evidence against a compensatory increase in prefrontal  
595 contribution to the task with age.

#### 596 *Testing sub-regions within PFC*

597 Again, we examined the four prefrontal subregions separately to assess whether the findings  
598 were driven by a specific part or parts of the large ROI (Table 5). For this experiment, the age-  
599 related increase in univariate activation was not separately significant in any subregion, which  
600 may have reflected relatively distributed effects and the more inclusive selection of ‘active’  
601 voxels. As for the LTM experiment however, overall age effects on the spread of multivariate  
602 voxel weights were significant in three subregions, and those in IFG were similar in magnitude  
603 and form, suggesting reductions in spread across PFC, with no major between-subregion  
604 differences. Moreover, all ROIs showed Bayes Factors of at least 6 against a boost to model  
605 evidence from adding PFC to the posterior-only models predicting increasing STM load, again  
606 consistent with the overall results.

ROI/ measure	Model		Linear			Quadratic		
	$F$	$P$	$t$	$r^2_{adj}$	$p$	$t$	$r^2_{adj}$	$p$
<b>BA10</b>								
Mean univariate	1.90	.155	1.79	--	.0787	-0.937	--	.352
MVB spread (SD)	12.7	< .0001	-1.41	--	.158	-4.69	.171	< .0001
PFC boost $t$	--	--	-1.48	--	.142	-1.00	--	.320
PFC boost $BF_{01}$	--	--	10.0	--	--	--	--	--
<b>IFG</b>								
Mean univariate	2.64	.0767	1.99	--	.0512	0.997	--	.323
MVB spread (SD)	6.26	.00282	-0.787	--	.427	-3.35	.0864	.00109
PFC boost $t$	--	--	-1.11	--	.270	-1.10	--	.274
PFC boost $BF_{01}$	--	--	7.69	--	--	--	--	--

<b>MFG</b>								
Mean univariate	2.08	.131	2.03	--	.0459	-0.447	--	.654
MVB spread (SD)	11.0	< .0001	0.300	--	.762	-4.60	.165	< .0001
PFC boost $t$	--	--	-1.38	--	.171	-0.788	--	.433
PFC boost $BF_{01}$	--	--	6.25	--	--	--	--	--
<b>SFG</b>								
Mean univariate	2.64	.0770	2.27	--	.0264	0.241	--	.812
MVB spread (SD)	7.37	.00106	-1.57	--	.116	-3.34	.0858	.00111
PFC boost $t$	--	--	-2.73	.0528	.00755	-0.720	--	.473
PFC boost $BF_{01}$	--	--	14.3	--	--	--	--	--

607 **Table 5.** Age effects for PFC subregions in the visual short-term memory task. The table lists mean  
608 univariate activation during maintenance in response to increasing VSTM load, the spread (SD) of  
609 MVB voxel weights predicting linearly increasing VSTM load, and results of the between-region tests  
610 of 'boost' to model evidence for PFC plus PVC models compared to PVC-only. See text for details.  
611 Alpha = .0125. SD = standard deviation. n=96.

612

### 613 *Testing posterior-anterior shift*

614 Finally, even if age increased activity and decreased multivariate information in both PFC and  
615 PVC, it is possible that the PFC:PVC ratio of activity and/or multivariate information increases  
616 with age, consistent with the general PASA claim. As for LTM encoding, there was no evidence  
617 that age effects on (univariate) activation in the two ROIs differed, i.e. the increase in activation  
618 in older people was similar in magnitude (Table 4;  $BF_{01}$  for null hypothesis over prediction of  
619 a greater age-related increase in PFC = 33.3). However, multivariate analysis revealed a  
620 picture different from that in the LTM task. In the separate MVB models, the age-related  
621 reduction in spread of weights showed a stronger quadratic component in PFC than PVC (for  
622 PFC-PFC, quadratic  $t(95) = 2.26$ ,  $p = .0244$ ; Table 4). More clearly, when examining the  
623 location of top-weighted voxels from the joint PFC+PVC model, a higher proportion were  
624 located in PFC in older age (for model,  $F(2,93) = 22.4$ ,  $p < .0001$ , linear  $t(95) = 3.72$ ,  $p < .001$ ,  
625 quadratic  $t(95) = 5.20$ ,  $p < .0001$ ), with mean 69.1% of top voxels located in PFC in the younger  
626 tertile (SD = 14.1; 25-43 years) but 81.0% in the older tertile (SD = 13.3; 66-85 years). Thus  
627 while the STM experiment, like the LTM experiment, found decreases in absolute PFC (and  
628 PVC) involvement in old age, the relative involvement of PFC versus PVC voxels (at least in  
629 terms of those with high weights in the joint model) did increase with age, unlike in the LTM  
630 experiment. This provides some support for a PASA pattern in this task, even though there  
631 was no evidence that this greater PFC involvement was compensatory.

## 632 Discussion

633 This study investigated the proposal that there is a posterior-to-anterior shift in task-related  
634 brain activity during aging, with the greater reliance on prefrontal cortex in older age reflecting  
635 compensatory mechanisms. We tested the predictions of this PASA theory with data from two  
636 memory tasks that were conducted on independent and relatively large population-derived  
637 adult lifespan samples. Using novel model-based multivariate analyses, we provide direct  
638 evidence against a compensatory posterior-to-anterior shift. Instead, our data suggest that the  
639 increased prefrontal activation reflects less specific or less efficient activity, rather than  
640 compensation.

641 The results of our standard univariate activation analyses are consistent with previous studies  
642 showing age-related increases in activation in prefrontal cortex, which form the basis of the  
643 PASA theory (Grady et al., 1994; Davis et al., 2008). Many studies have found such increases  
644 in PFC activation in different cognitive tasks, although regional reductions in activation are  
645 also found (e.g. see Rajah and D'Esposito, 2005; Spreng et al., 2010; Li et al., 2015). We  
646 found such age-related increases in both the PFC activation associated with trials that were  
647 later remembered many minutes later (in the LTM experiment) and the activation associated  
648 with maintaining increasing numbers of items for a few seconds (in the STM experiment). We  
649 also further generalized previous findings across PFC sub-regions, in that the increased  
650 activation was reliable across lateral, anterior and superior prefrontal areas (although in the  
651 LTM experiment, it was mainly driven by inferolateral and anterior PFC).

652 Importantly, despite this increased univariate activity, multivariate analysis of both  
653 experiments showed that with increasing age, PFC possessed less, rather than more,  
654 information about the cognitive outcome. This reduced pattern information was evident both  
655 in terms of the spread of voxel weights (Figure 2) and the lack of a meaningful boost to model  
656 evidence when adding PFC voxels to the model (Figure 3). The latter type of inference was  
657 made possible by our novel use of multivariate Bayesian (MVB) classification.

658 If the increased prefrontal activation with age is not compensatory, then what does it reflect?  
659 One possibility is that neural function is less efficient, such that a greater BOLD signal is  
660 required for the same level of computation, i.e, less "bang for the buck" for the same level of  
661 neural activity (Grady, 2008; see also Rypma and Esposito, 2000; Morcom et al., 2007;  
662 Reuter-Lorenz and Campbell, 2008; Nyberg et al., 2014). This could reflect the proposed  
663 greater sensitivity of prefrontal cortices than other brain regions to aging (West, 1996; Glisky  
664 et al., 2001; Raz and Rodrigue, 2006). Another possibility is that PFC activity becomes less  
665 specific with age, as might be expected by theories of age-related dedifferentiation, particularly  
666 in complex cognitive functions (Li et al., 2001; Park et al., 2004; Carp et al., 2011;

667 Abdulrahman et al., 2014). Partial support for the latter comes from the LTM experiment,  
668 where the negative effect of age on the spread of multivariate weights across voxels was  
669 accompanied by a positive effect of age on the spread (as well as mean) of univariate activity.  
670 This suggests that, while more voxels showed substantial (positive or negative) activity related  
671 to subsequent memory in older people, these additional responses were redundant, with fewer  
672 voxels contributing uniquely to memory encoding, as expected if the increased prefrontal  
673 activity is less specific. In the STM experiment, on the other hand, the spread of univariate  
674 responses was age-invariant, suggesting a more spatially uniform increase in response to  
675 load with age, although the MVB results suggested that – just as in the LTM task – this  
676 increased response carried less information. Whether the present results reflect reductions in  
677 efficiency or reductions in specificity, they are more consistent with the general idea of brain  
678 maintenance (Nyberg et al., 2014) – that cognitive function in older age is determined by the  
679 ability to maintain a youth-like brain – than with the idea associated with PASA of functional  
680 compensation by anterior brain regions.

681 Despite age-related decreases in overall multivariate information in both PFC and PVC, it is  
682 possible that the *relative* contribution of anterior regions to cognitive tasks could increase with  
683 age. There is some evidence for such a shift from studies showing crossover effects in which  
684 age-related decreases in posterior cortical activity occur alongside age-related increases in  
685 PFC (e.g., Grady et al., 1994; Davis et al., 2008; see also recent meta-analysis by Maillet and  
686 Rajah, 2014). However, our univariate activation analyses showed little evidence of such a  
687 relative posterior-to-anterior shift: despite increased prefrontal activation, age effects on  
688 univariate activation in PFC and PVC did not differ significantly in either experiment. In terms  
689 of multivariate information, the LTM experiment actually showed, if anything, a decrease rather  
690 than increase in the contribution of PFC relative to PVC. The only comparison that provided  
691 some support for a relative increase in anterior contribution was for multivariate information  
692 about load in the STM experiment. Thus the direction of any *relative* shift in reliance on PFC  
693 versus PVC with age seems to be task-dependent, as opposed to the task-general posterior-  
694 to-anterior shift claimed by PASA (Davis et al., 2008; see also Ford and Kensinger, 2017).  
695 This is consistent with other meta-analyses, which have found age-related decreases as well  
696 as increases in activation, depending on the task (Spreng, Wojtowicz, & Grady, 2010; Li et al.,  
697 2015). Moreover, most studies have not made the direct statistical comparisons needed to  
698 test for anterior-posterior differences in the absence of crossover effects (see Morcom &  
699 Johnson, 2015). A strength of our approach is that our analyses encompassed large ROIs in  
700 both anterior and posterior cortices, as well as direct comparisons between the two.

701 In summary, our data replicate an increase in PFC activity over the adult lifespan, but do not  
702 support the idea that this reflects a compensatory posterior-to-anterior shift, at least in the



703 context of the two memory tasks considered here. Our results are inconsistent both with the  
704 proposal that the increased activity is compensatory, and with a generalized shift with age to  
705 greater relative reliance on prefrontal cortex. The data are most parsimoniously explained by  
706 reduced efficiency or specificity of neural responses, reflecting primary age-related deleterious  
707 changes in posterior as well as prefrontal cortex which vary in their relative magnitudes  
708 according to the task. Our results therefore help to adjudicate between competing accounts of  
709 neurocognitive aging, while also illustrating the more general ability of MVB to compare  
710 models that comprise different sets of voxels, thereby offering an exciting new general way to  
711 test the relative contributions of brain regions to cognitive outcomes.

## 712 Acknowledgments

713 A.M.M. is a member of the University of Edinburgh Centre for Cognitive Ageing and Cognitive  
714 Epidemiology (CCACE), part of the UK cross-council Lifelong Health and Wellbeing Initiative,  
715 Grant number G0700704/84698. The Cambridge Centre for Ageing and Neuroscience (Cam-  
716 CAN) research was supported by the Biotechnology and Biological Sciences Research  
717 Council (grant number BB/H008217/1). The full Cam-CAN author list can be found here:  
718 <http://www.cam-can.org/index.php?content=corpauth>. R.N.A.H. is funded by the Medical  
719 Research Council (SUAG/010 RG91365) with additional support by the European Union's  
720 Horizon 2020 research and innovation programme (grant agreement No 732592).

## 721 Author contributions

722 A.M.M. designed research; A.M.M., R.N.A.H. and Cam-CAN performed research; A.M.M. and  
723 R.N.A.H. analyzed data; A.M.M. and R.N.A.H. wrote the paper.

## 724 References

- 725 Abdulrahman H, Fletcher PC, Bullmore E, Morcom AM (2014) Dopamine and memory  
726 dedifferentiation in aging. *Neuroimage*.
- 727 Ashburner J (2007) A fast diffeomorphic image registration algorithm. 38:95–113.
- 728 Ashburner J, Friston KJ (2005) Unified segmentation. *Neuroimage* 26:839–851.
- 729 Cabeza R, Daselaar SM, Dolcos F, Prince SE, Budde M, Nyberg L (2004) Task-independent  
730 and Task-specific Age Effects on Brain Activity during Working Memory, Visual Attention  
731 and Episodic Retrieval. *Cereb Cortex* 14:364–375.
- 732 Cappell KA, Gmeindl L, Reuter-lorenz PA (2010) Age differences in prefrontal recruitment  
733 during verbal working memory maintenance depend on memory load. *CORTEX* 46:462–  
734 473 Available at: <http://dx.doi.org/10.1016/j.cortex.2009.11.009>.

- 735 Carp J, Park J, Polk TA, Park DC (2011) Age differences in neural distinctiveness revealed by  
736 multi-voxel pattern analysis. *Neuroimage* 56:736–743 Available at:  
737 <http://dx.doi.org/10.1016/j.neuroimage.2010.04.267>.
- 738 Chadwick MJ, Bonnici HM, Maguire EA (2012) Decoding information in the human  
739 hippocampus: A user's guide. *Neuropsychologia* 50:3107–3121 Available at:  
740 <http://dx.doi.org/10.1016/j.neuropsychologia.2012.07.007>.
- 741 Chadwick MJ, Bonnici HM, Maguire EA (2014) CA3 size predicts the precision of memory  
742 recall. *Proc Natl Acad Sci* 111:10720–10725 Available at:  
743 [http://www.pubmedcentral.nih.gov/articlerender.fcgi?artid=4115494&tool=pmcentrez&re](http://www.pubmedcentral.nih.gov/articlerender.fcgi?artid=4115494&tool=pmcentrez&rendertype=abstract)  
744 [ndertype=abstract](http://www.pubmedcentral.nih.gov/articlerender.fcgi?artid=4115494&tool=pmcentrez&rendertype=abstract).
- 745 Davis SW, Dennis NA, Daselaar SM, Fleck MS, Cabeza R (2008) Que PASA? the posterior-  
746 anterior shift in aging. *Cereb Cortex* 18:1201–1209.
- 747 Dienes Z (2014) Using Bayes to get the most out of non-significant results. *Front Psychol* 5:1–  
748 17.
- 749 Emrich SM, Riggall AC, LaRocque JJ, Postle BR (2013) Distributed Patterns of Activity in  
750 Sensory Cortex Reflect the Precision of Multiple Items Maintained in Visual Short-Term  
751 Memory. *J Neurosci* 33:6516–6523 Available at:  
752 <http://www.jneurosci.org/cgi/doi/10.1523/JNEUROSCI.5732-12.2013>.
- 753 Ford JH, Kensinger EA (2017) Age-Related Reversals in Neural Recruitment across Memory  
754 Retrieval Phases. *J Neurosci*:0521–17 Available at:  
755 <http://www.jneurosci.org/lookup/doi/10.1523/JNEUROSCI.0521-17.2017>.
- 756 Friston K, Chu C, Mourao-Miranda J, Hulme O, Rees G, Penny W, Ashburner J (2008)  
757 Bayesian decoding of brain images. *Neuroimage* 39:181–205.
- 758 Friston K, Mattout J, Trujillo-Barreto N, Ashburner J, Penny W (2007) Variational free energy  
759 and the Laplace approximation. *Neuroimage* 34:220–234.
- 760 Glisky EL, Rubin SR, Davidson PSR (2001) Source Memory in Older Adults : An Encoding or  
761 Retrieval Problem ? *J Neurosci* 21:1131–1146.
- 762 Grady C (2012) The cognitive neuroscience of ageing. *Nat Rev Neurosci* 13:491–505  
763 Available at: <http://www.ncbi.nlm.nih.gov/pubmed/22714020>.
- 764 Grady CL, Maisog JM, Horwitz B, Ungerleider LG, Mentis MJ, Salerno JA, Pietrini P, Wagner  
765 E, Haxby J V (1994) Age-related changes in cortical blood flow activation during visual

- 766 processing of faces and location. *J Neurosci* 14:1450–1462.
- 767 Grady CL, Mcintosh AR, Bookstein F, Horwitz B, Rapoport SI, Haxby J V (1998) Age-Related  
768 Changes in Regional Cerebral Blood Flow during Working Memory for Faces. 425:409–  
769 425.
- 770 Henson RN et al. (2016) Multiple determinants of lifespan memory differences. *Sci Rep*  
771 6:32527 Available at: <http://www.nature.com/articles/srep32527>.
- 772 Hulme OJ, Skov M, Chadwick MJ, Siebner HR, Rams??y TZ (2014) Sparse encoding of  
773 automatic visual association in hippocampal networks. *Neuroimage* 102:458–464  
774 Available at: <http://dx.doi.org/10.1016/j.neuroimage.2014.07.020>.
- 775 Lancaster JL, Woldorff MG, Parsons LM, Liotti M, Freitas CS, Rainey L, Kochunov P V.,  
776 Nickerson D, Mikiten SA, Fox PT (2000) Automated Talairach Atlas labels for functional  
777 brain mapping. *Hum Brain Mapp* 10:120–131.
- 778 Lang PJ, Bradley MM, Cuthbert BN (1997) International Affective Picture System (IAPS):  
779 Technical Manual and Affective Ratings. *NIMH Cent Study Emot Atten*:39–58 Available  
780 at:  
781 [http://www.unifesp.br/dpsicobio/adap/instructions.pdf%5Cnhttp://econtent.hogrefe.com/  
782 doi/abs/10.1027/0269-8803/a000147](http://www.unifesp.br/dpsicobio/adap/instructions.pdf%5Cnhttp://econtent.hogrefe.com/doi/abs/10.1027/0269-8803/a000147).
- 783 Li H-J, Hou X-H, Liu H-H, Yue C-L, Lu G-M, Zuo X-N (2015) Putting age-related task activation  
784 into large-scale brain networks: A meta-analysis of 114 fMRI studies on healthy aging.  
785 *Neurosci Biobehav Rev* 57:156–174.
- 786 Li S-C, Li S-C, Lindenberger U, Lindenberger U, Sikstrom S, Sikstrom S (2001) Aging  
787 cognition: From neuromodulation to representation. 5:479–486.
- 788 Maass A, Schütze H, Speck O, Yonelinas A, Tempelmann C, Heinze H-J, Berron D,  
789 Cardenas-Blanco A, Brodersen KH, Enno Stephan K, Düzel E (2014) Laminar activity in  
790 the hippocampus and entorhinal cortex related to novelty and episodic encoding. *Nat*  
791 *Commun* 5:5547 Available at:  
792 [http://www.nature.com/doi/10.1038/ncomms6547%5Cnhttp://www.pubmedcentral.  
793 nih.gov/articlerender.fcgi?artid=4263140&tool=pmcentrez&rendertype=abstract](http://www.nature.com/doi/10.1038/ncomms6547%5Cnhttp://www.pubmedcentral.nih.gov/articlerender.fcgi?artid=4263140&tool=pmcentrez&rendertype=abstract).
- 794 Maillet D, Rajah MN (2014) Age-related differences in brain activity in the subsequent memory  
795 paradigm: A meta-analysis. *Neurosci Biobehav Rev* 45:246–257 Available at:  
796 <http://dx.doi.org/10.1016/j.neubiorev.2014.06.006>.

- 797 Maldjian JA, Laurienti PJ, Kraft RA, Burdette JH (2003) An automated method for  
798 neuroanatomic and cytoarchitectonic atlas-based interrogation of fMRI data sets.  
799 *Neuroimage* 19:1233–1239.
- 800 Morcom AM, Friston KJ (2012) Decoding episodic memory in ageing: A Bayesian analysis of  
801 activity patterns predicting memory. *Neuroimage* 59.
- 802 Morcom AM, Good CD, Frackowiak RSJ, Rugg MD (2003) Age effects on the neural correlates  
803 of successful memory encoding. *Brain* 126.
- 804 Morcom AM, Johnson W (2015) Neural reorganization and compensation in aging. *J Cogn  
805 Neurosci* 27.
- 806 Morcom AM, Li J, Rugg MD (2007) Age effects on the neural correlates of episodic retrieval:  
807 Increased cortical recruitment with matched performance. *Cereb Cortex* 17.
- 808 Nyberg L, Andersson M, Kauppi K, Lundquist A, Persson J, Pudas S, Nilsson LG (2014) Age-  
809 related and genetic modulation of frontal cortex efficiency. *J Cogn Neurosci* 26:746–764.
- 810 Nyberg L, Lövdén M, Riklund K, Lindenberger U, Bäckman L (2012) Memory aging and brain  
811 maintenance. *Trends Cogn Sci* 16:292–305.
- 812 Park DC, Polk TA, Park R, Minear M, Savage A, Smith MR (2004) Aging reduces neural  
813 specialization in ventral visual cortex. *J Cogn Neurosci* 16:13091–13095.
- 814 Park DC, Reuter-Lorenz P (2009) The adaptive brain: aging and neurocognitive scaffolding.  
815 *Annu Rev Psychol* 60:173–196 Available at:  
816 <http://www.ncbi.nlm.nih.gov/pubmed/19035823>.
- 817 Rajah MN, D'Esposito M (2005) Region-specific changes in prefrontal function with age: A  
818 review of PET and fMRI studies on working and episodic memory. *Brain* 128:1964–1983.
- 819 Raz N, Rodrigue KM (2006) Differential aging of the brain: Patterns, cognitive correlates and  
820 modifiers. *Neurosci Biobehav Rev* 30:730–748.
- 821 Reuter-Lorenz PA, Campbell KA (2008) Neurocognitive ageing and the Compensation  
822 Hypothesis. *Curr Dir Psychol Sci* 17:177–182.
- 823 Rouder JN, Speckman PL, Sun D, Morey RD, Iverson G (2009) Bayesian t tests for accepting  
824 and rejecting the null hypothesis. *Psychon Bull Rev* 16:225–237.
- 825 Rypma B, Esposito MD (2000) Isolating the neural mechanisms of age-related changes in  
826 human working memory. *J Cogn Neurosci* 12:509–515.

- 827 Shafto M a, Tyler LK, Dixon M, Taylor JR, Rowe JB, Cusack R, Calder AJ, Marslen-Wilson  
828 WD, Duncan J, Dalgleish T, Henson RN, Brayne C, Matthews FE (2014) The Cambridge  
829 Centre for Ageing and Neuroscience (Cam-CAN) study protocol: a cross-sectional,  
830 lifespan, multidisciplinary examination of healthy cognitive ageing. *BMC Neurol* 14:204  
831 Available at:  
832 [http://www.pubmedcentral.nih.gov/articlerender.fcgi?artid=4219118&tool=pmcentrez&re](http://www.pubmedcentral.nih.gov/articlerender.fcgi?artid=4219118&tool=pmcentrez&rendertype=abstract)  
833 [ndertype=abstract](http://www.pubmedcentral.nih.gov/articlerender.fcgi?artid=4219118&tool=pmcentrez&rendertype=abstract).
- 834 Smith APR, Henson RNA, Dolan RJ, Rugg MD (2004) fMRI correlates of the episodic retrieval  
835 of emotional contexts. *Neuroimage* 22:868–878.
- 836 Spreng RN, Wojtowicz M, Grady CL (2010) Reliable differences in brain activity between  
837 young and old adults: A quantitative meta-analysis across multiple cognitive domains.  
838 *Neurosci Biobehav Rev* 34:1178–1194 Available at:  
839 <http://dx.doi.org/10.1016/j.neubiorev.2010.01.009>.
- 840 Taylor JR, Williams N, Cusack R, Auer T, Shafto MA, Dixon M, Tyler LK, Cam-CAN X, Henson  
841 RN (2015) The Cambridge Centre for Ageing and Neuroscience (Cam-CAN) data  
842 repository: Structural and functional MRI, MEG, and cognitive data from a cross-sectional  
843 adult lifespan sample. *Neuroimage* 144:262–269 Available at:  
844 <http://dx.doi.org/10.1016/j.neuroimage.2015.09.018>.
- 845 Tzourio-Mazoyer N, Landeau B, Papathanassiou D, Crivello F, Etard O, Delcroix N, Mazoyer  
846 B, Joliot M (2002) Automated anatomical labeling of activations in SPM using a  
847 macroscopic anatomical parcellation of the MNI MRI single-subject brain. *Neuroimage*  
848 15:273–289.
- 849 Venables WN (William N., Ripley BD, Venables WN (William N). (2002) *Modern applied*  
850 *statistics with S*.
- 851 Wagenmakers E-J (2007) A practical solution to the pervasive problems of p values. 14:779–  
852 804.
- 853 West RL (1996) An application of prefrontal cortex function theory to cognitive aging. *Psychol*  
854 *Bull* 120:272–292.